# Focusing performance of small $f$-number metallic lens with depth-modulated slits*

Gao Yang(高 扬), Zhang Xue-Ru(张学如)†, Wang Yu-Xiao(王玉晓), Song Ying-Lin(宋瑛林), and Liu Shu-Tian(刘树田)

*Department of Physics, Harbin Institute of Technology, Harbin* 150001, *China*

(Received 29 March 2010; revised manuscript received 1 May 2010)

This paper studies a small $f$-number metallic lens with depth-modulated slits. Slits filled with dielectric between silver plates are designed to produce desired optical phase retardations based on the particular propagation properties of surface plasmon polaritons in nanostructures. Numerical simulation of this structure is performed through the finite-difference time-domain method. Different from the conventional dielectric lens, the metallic lens can be used as a pure phase element without energy loss brought by the light refraction at curved surfaces and total internal reflection. The focusing performance is consequently improved, with larger diffraction efficiency than that of the same shaped dielectric lens.

**Keywords:** surface plasmon polaritons, subwavelength structures, finite-difference time-domain

**PACC:** 4225B, 4230, 7320M

## 1. Introduction

Optical resolution restricts the development of the imaging for the conventional lens due to the diffraction nature of electromagnetic waves. This limit seems to be broken by the so-called superlens which is constructed by a slab of negative refractive index material[1] and certified experimentally soon later.[2,3] Recently, researchers have paid much more attention than ever before to the research of the subwavelength imaging theoretically and experimentally.[4−13] Various plasmonic structures have been proposed to concentrate light in subwavelength scale.[9−17] Among them, the metallic nano-slit array structure, which supports subwavelength surface plasmon modes, provides important new opportunities and flexibilities for manipulating light at the subwavelength scale. Electromagnetic wave transmits through these nano-slits which provide the desired phase retardations of beam manipulating by adjusting structure and/or material parameters of nano-slits, such as the dielectric constant in the slit region, slit width[13] or slit depth.[11,14] Shi *et al.*[11] proposed a focusing structure using a single metallic slit surrounded with depth-modulated grooves. However, the transmittance is limited for the single-slit configuration. The analysis of Sun *et al.*[14] shows refractive transmission of light through the nano-slit array, claiming the possibility of realizing the beam shaping based on the refractive optics. However, the bulk lens[14] cannot be regarded as a pure phase element for the finite thickness. In this paper, we focused on the construction of pure phase elements using the metallic slit arrays.

Small $f$-number lenses are useful for super high resolution.[18] To construct a small $f$-number dielectric lens, higher surface curvature and refractive index material are required, which will consequently lower the energy transmittance and increase the energy loss due to the total internal reflection. In this paper, we employ a metallic plate with depth-modulated slits to realize extremely small $f$-number focusing. The finite-difference time-domain (FDTD) method is used to investigate the focusing performances, such as the real focal length, the focal depth range, the focal spot size, and the diffraction efficiency. As comparison, the focusing performances of the conventional dielectric lens with the same parameters are also investigated.

This paper is organized as follows. Section 2 of this paper will present the principle of phase modulation by varying slit depth and the design methodology of the small $f$-number metallic lens. The subjects of discussion in Section 3 are numerical simulation and analysis of this structure. A brief conclusion is given in Section 4.

*Project supported by the National Basic Research Program of China (Grant No. 2006CB302901) and the Foundation of the Ministry of Science and Technology of China for the International Collaboration on Scientific Research (Grant No. 2009DFA50620).

†Corresponding author. E-mail: xrzhang@hit.edu.cn

© 2010 Chinese Physical Society and IOP Publishing Ltd

# 2. Principles

## 2.1. Phase modulation by metallic slits

First, we review the process of light transmission through the nano-slits of the metallic structure. Surface plasmon polaritons (SPPs) can be excited at the slit entrance when a TM polarized incident plane wave impinges the slit entrance and SPPs can propagate along metallic surfaces while keeping bounded near the surface without radiation away.[19,20] Some of the SPPs propagate inside the slits with a complex propagation constant in the specific guided modes until reaching the export where they diffract into all radial directions with a uniform power distribution.

Considering a single nano-slit as shown in Fig. 1(a), the SPPs excited will be coupled and propagated in the form of a guided mode for the TM polarized case. The complex propagation constant $\beta$ can be calculated from[21]

$$\tanh\left(\sqrt{\beta^2 - k_0^2\varepsilon_{\rm d}}\,\frac{w}{2}\right) = \frac{-\varepsilon_{\rm d}\sqrt{\beta^2 - k_0^2\varepsilon_{\rm m}}}{\varepsilon_{\rm m}\sqrt{\beta^2 - k_0^2\varepsilon_{\rm d}}}, \quad (1)$$

where $k_0$ is the wave vector of light in vacuum, $\varepsilon_{\rm m}$ and $\varepsilon_{\rm d}$ are the relative dielectric constant for the metal and the material inside the slit respectively, and $w$ is the slit width. Effective refractive index of the fundamental mode inside the slit is expressed as $n_{\rm eff} = \beta/k_0$. In this paper, silver with $\varepsilon_{\rm m} = -18.938 + {\rm i}\,0.213$ at the incident wavelength of 650 nm is used.[22] Variations of the effective refractive indices with the dielectric constant $n$ of the filled material and the slit width $w$ are calculated and shown in Figs. 1(b) and 1(c). From the figures, it is clear that $n_{\rm eff}$ highly depends on the filled material and the slit width. It also needs to be mentioned that the effective index of the guided mode in the slit is higher than the actual index of the filled dielectric material. This agrees with the slow wave properties of SPPs,[23] and it is quite different from the case at X band where the effective index is lower than that of the filled material between the two metal plates.[24]

For a metallic slit with finite length $h$, the phase change of light transmitted can be written as[25]

$$\Delta\Phi = \Delta\varphi_1 + \Delta\varphi_2 = {\rm Re}(k_0 n_{\rm eff} h) + \arg\left[1 - \left(\frac{1-\beta/k_0}{1+\beta/k_0}\right)^2 \exp({\rm i}\,2\beta h)\right], \quad (2)$$

where $\Delta\varphi_1$ is the phase retardation of SPPs propagation in the slit and $\Delta\varphi_2$ originates from the multiple reflections between the entrance and exit interfaces. Strictly speaking, equation (2) should include the phase changes contributed by the coupling of SPPs at the entrance and the exit interfaces. However, for the metallic lens design in this paper, all these parts could be ignored in comparison with the dominant phase change $\Delta\varphi_1$.

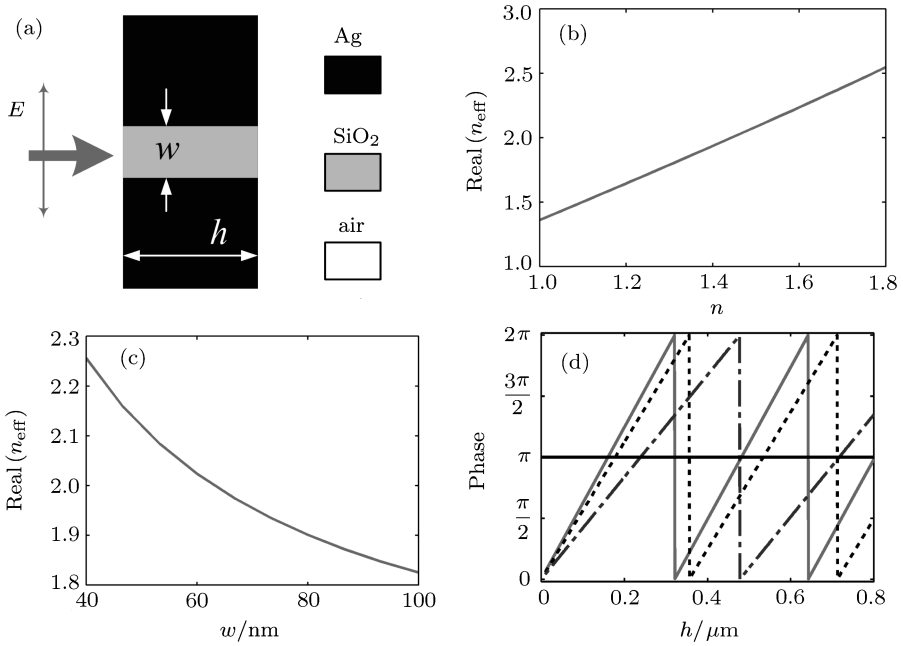



**Fig. 1.** (a) A schematic diagram of a single Ag/$SiO_2$/Ag slit, $w$ is slit width, $h$ is slit depth. (b) The real part of the effective index $n_{\rm eff}$ as a function of filled material ($n$) for the slit width $w = 60$ nm. (c) The real part of the effective index $n_{\rm eff}$ as a function of slit width $w$. The filled material is $SiO_2$ ($n = 1.46$). (d) The phase modulation of light as a function of slit depth $h$ for the Ag/$SiO_2$/Ag slit with $w = 60$ nm (solid line), Ag/$SiO_2$/Ag slit with $w = 100$ nm (dotted line), and Ag/Air/Ag slit with $w = 60$ nm (dash-dotted line), respectively.

From Eq. (2), phase modulation of light transmitting through slits can be realized by changing the effective index $n_{\text{eff}}$ or adjusting the slit depth $h$. The phase change as a function of the slit depth $h$ for different kinds of slits are calculated according to Eq. (2) and depicted in Fig. 1(d). From the figure, it can be seen that the slit with the smallest width and filled with high refractive index material has the deepest phase modulation. Considering the requirement of the design of small $f$-number metallic lens and based on the computation results depicted in Fig. 1, we set the slit width as $w = 60$ nm and $SiO_2$ as the filled material.

### 2.2. Design metallic lens with small $f$-number

Figure 2(a) shows the design scheme where the lens is considered as a pure phase element. Light illuminates on the convex surface and there is no refraction at the interface between the element and air. The preset focal length is $f_0$. The profile of the curved surface can be expressed as the following equation

$$y(x) = \frac{n_2}{n_1 - n_2}\left(\sqrt{f_0^2 + x^2} - f_0\right), \tag{3}$$

where $n_1$ and $n_2$ are the refractive index of the lens and the circumstance, respectively. Here, $n_1$ should be greater than $n_2$, which is required for focusing light.

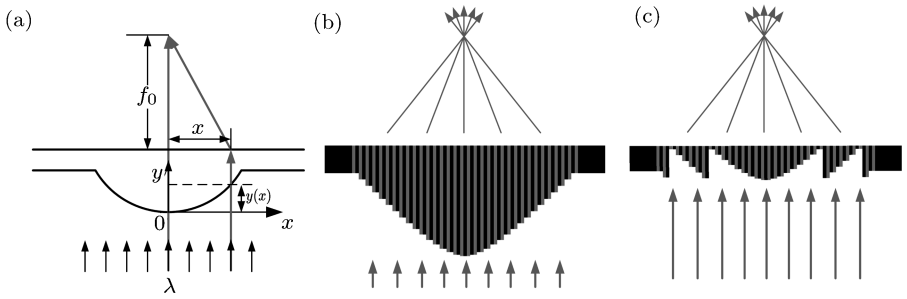



**Fig. 2.** (a) Original design scheme of a pure phase lens. (b) and (c) Schemes of the metallic lens without and with fresnelization respectively.

To construct metallic lens, we use silver as the metal material. The $D = 4$ $\mu$m is the diameter of the lens aperture and $f_0 = 600$ nm is the preset focal length. The $f$-number is then $f/\# = f_0/D = 0.15$. For a metallic slit with width 60 nm and filled with $SiO_2$, the effective index is $n_{\text{eff}} = 2.024$ for the incident wavelength 650 nm. The circumstance material is air with a constant refractive index $n_2 = 1$. To realize phase modulation, nano-slits are realized by alternately stacking silver and $SiO_2$ plates. According to Eq. (3) and setting $n_1 = 2.024$, $n_2 = 1$, we design the metallic lens and depict it in Fig. 2(b). Here, slit space is set to be 60 nm which is bigger than the double skin depth to neglect the SPPs coupling between the adjacent slits. The metallic lens is regarded as a pure phase element. There is no refraction at the curved surface, which is quite different from the traditional dielectric lens.

Next, reducing the thickness of the metallic lens from 2 $\mu$m to 600 nm we used the Fresnel theory[25] to optimize the lens (as depicted in Fig. 2(c)). There are several advantages as the followings for this optimization. The size of the metallic lens is miniaturized. Fabrication process of the slits may be relatively easy because of the shortened thickness of the structure. The energy loss of light transmitting through the slits decreases accordingly. The diffraction efficiency is correspondingly enhanced.

## 3. Numerical simulation and analysis

### 3.1. Numerical simulation

FDTD simulations are performed to explore the focusing performance of the designed metallic lens. The simulation region size is 4 $\mu$m×5 $\mu$m with uniform discrete grids of $\Delta x = \Delta y = 2$ nm. A perfect matched layer[26] is used as the boundary condition. A source line which is parallel with the lens is placed in front of the

curved surface. After 20000 steps of calculation, the steady optical field (the magnetic intensity distribution $|H_z|^2$) of the simulation result is obtained and shown in Fig. 3(a). From the figure, it can be seen that a clear-cut focus appears away from the exit surface of the metallic lens. The intensity distribution on the axis is extracted and depicted in Fig. 3(b). The real focal length is about 648 nm and the relative deviation from the preset focal length $f_0 = 600$ nm is 8.0%. This result definitely verifies the feasibility of the metallic lens for small $f$-number. The shift of the focal length, we believe, is due to the discrete distribution of slits and the SPPs coupling between the slits.

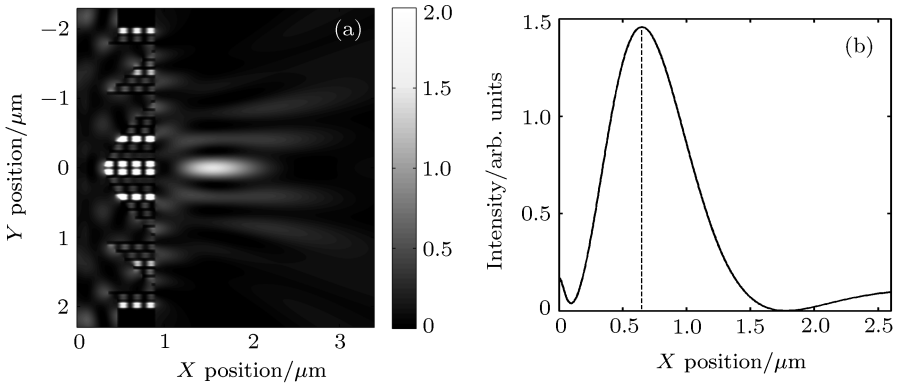



**Fig. 3.** (a) Calculated steady magnetic field intensity $|H_z|^2$ of the simulation results of the metallic lens using FDTD method. (b) Axial intensity distribution extracted from (a).

## 3.2. Comparison with dielectric lens

To further demonstrate the efficiency of metallic lens in small $f$-number focusing, the focusing performances of the metallic lens and the dielectric lens are compared. The dielectric index of lens material is set as $n_1 = 2.024$ which is the same as the real part of the effective index of the SPP mode in the metallic slit. The lens shape is kept the same with the metallic lens. Figure 4(a) shows the FDTD simulation results of the optical transmission with incidence at the curved surface. The aperture is limited to $D = 4$ $\mu$m being the same with the metallic lens. The axial intensity distribution is depicted in Fig. 4(b). The real focal length is about 514 nm and the relative deviation from the preset focal length is 14.3%. This substantial deviation is due to the strong refraction effect which is caused by the high refractive index material and large curvature at the front surface. It means that the dielectric lens with an incidence at the curved surface cannot be considered as a pure phase element in the case of small $f$-number.

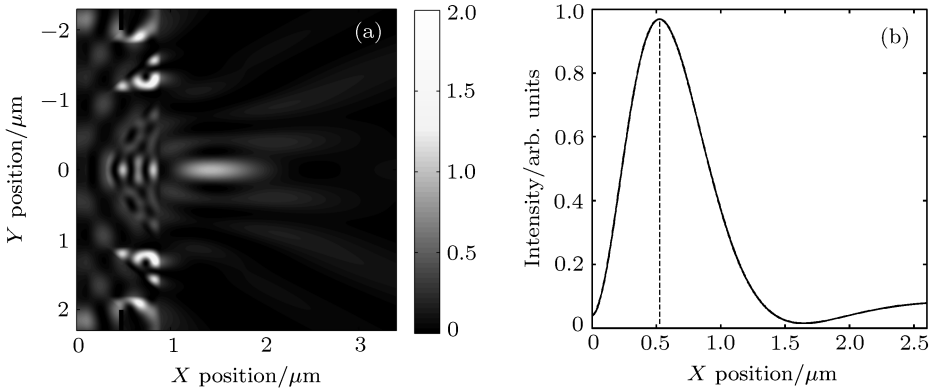



**Fig. 4.** (a) Calculated steady magnetic field intensity $|H_z|^2$ of the simulation results of the dielectric lens using FDTD method. (b) Axial intensity distribution extracted from (a).

Other focusing performances are also investigated. The lateral intensity profiles of the designed metallic lens and dielectric lens on the focal planes are presented in Fig. 5, respectively. The focal spot sizes, which are represented by the full width at half maximum (FWHM), are 234 nm and 246 nm, both are approximately one third of the incident wavelength. The diffraction efficiency, which is defined as the percentage ratio of the focused power in the main lobe to the total incident power, is 69.1% for the metallic lens. The fraction of slits area is 50% for the metallic lens. Obviously, this high diffraction efficiency is mainly due to the SPPs. The diffraction efficiency for the dielectric lens is 48.3%. The low focusing efficiency is due to the total internal reflection in the high order Fresnel zone, which is clearly shown in Fig. 4(a). Comparison of more detailed focusing performance is listed in Table 1. The focal depth is defined as FWHM in the axial plane. There are obvious advantages for metallic lens in comparison with the dielectric lens in polarization selectiveness and diffraction efficiency in the case of small $f$-number.

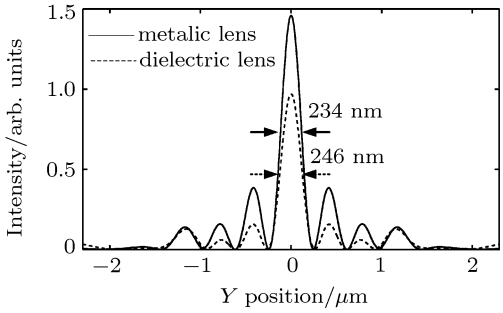



**Fig. 5.** Cross section at the real focal plane of the metallic lens (solid line) and the dielectric lens (dashed line).

**Table 1.** Comparison of focusing characteristics for the metallic lens and dielectric lens for $f/\# = 0.15$ (i.e., $f_0 = 600$ nm).

| type | polarization selectiveness | real focus length/nm | focal spot size/nm | diffraction efficiency/% | focus depth /nm |
|---|---|---|---|---|---|
| metallic lens | TM | 648 | 234 | 69.1 | 712 |
| dielectric lens | none | 514 | 246 | 48.3 | 698 |

## 4. Conclusion

Based on the transmission properties of SPPs, a specially designed metallic lens is used as a focusing device with small $f$-number. Numerical simulation using FDTD method illustrates a clear-focus spot with FWHM width about one third of the incident wavelength. Comparing with the conventional dielectric lens, we find that there is smaller shift of focal length due to the refraction at the curved surface and no energy loss contributed by the total internal reflection in the case of the metallic lens with small $f$-number. The enhanced diffraction efficiency involving SPPs is also observed. All these advantages show a path toward achieving miniaturization and enhancing the focusing performances of the metallic lens, which have great potential applications, such as photoetching, polarization imaging and nano-antenna.

## References

[1] Pendry J B 2000 *Phys. Rev. Lett.* **85** 3966
[2] Fang N, Lee H, Sun C and Zhang X 2005 *Science* **308** 534
[3] Melville D O S and Blaikie R J 2005 *Opt. Express* **13** 2127
[4] Jacob Z, Alekseyev L V and Narimanov E 2006 *Opt. Express* **14** 8247
[5] Salandrino A and Engheta N 2006 *Phys. Rev.* B **74** 075103
[6] Smolyaninov I I, Hung Y J and Davis C C 2007 *Science* **315** 1699
[7] Liu Z, Lee H, Xiong Y, Sun C and Zhang X 2007 *Science* **315** 1686
[8] Kim H, Hahn J and Lee B 2008 *Opt. Express* **16** 3049
[9] Wood B, Pendry J B and Tsai D P 2006 *Phys. Rev.* B **74** 115116
[10] Gorden R 2009 *Phys. Rev. Lett.* **102** 207402
[11] Shi H, Du C and Luo X 2007 *Appl. Phys. Lett.* **91** 093111
[12] Jung Y J, Park D, Koo S, Yu S and Park N 2009 *Opt. Express* **17** 397

[13] Shi H, Wang C, Du C, Luo X, Dong X and Gao H 2005 *Opt. Express* **13** 6815

[14] Sun Z and Kim H K 2004 *Appl. Phys. Lett.* **85** 642

[15] Wang L, Deng L, Cui N, Niu Y P and Gong S Q 2010 *Chin. Phys.* B **19** 017303

[16] Sun M, Liu R, Li Z, Cheng B, Zhang D, Yang H and Jin A 2006 *Chin. Phys.* **15** 1591

[17] Xue W, Guo Y and Zhang W 2009 *Chin. Phys.* B **18** 2529

[18] Herzig H P 1996 *Micro-optics: Elements, System and Application* (London: Taylor & Francis)

[19] Raether H 1988 *Surface Plasmons on Smooth and Rough Surface and on Gratings* (Heidelber: Springer)

[20] Barnes W L, Dereux A and Ebbesen T W 2003 *Nature* **424** 824

[21] Gordon R and Brolo A G 2005 *Opt. Express* **13** 1933

[22] Johnson P B and Christy R W 1972 *Phys. Rev.* B **12** 4370

[23] Feigenbaum E and Orenstein M 2007 *J. Lightwave Technol.* **25** 2547

[24] Matsushima A, Nakamura Y and Tomino S 2005 *Prog. Electromagn. Res.* **54** 245

[25] Born M and Wolf E 1999 *Principles of Optics* 7th edn. (Cambridge: Cambridge University Press)

[26] Taflove A and Hagness S C 2000 *Computational Electrodynamics: The Finite-Difference Time-Domain Method* 2nd edn. (Boston: Artech House)